JOURNAL OF SUSTAINABLE ENGINEERING AND TECHNOLOGY

Journal homepage: www.joset.com.ng

Characterization and Optimization of Concrete Properties Blended with Sesame Straw Ash as a Partial Replacement of Cement by Response Surface Methodology

Tasiu Ashiru Sulaiman[1], Yusuf Yau[1], Isah Garba[1]., Abdurrahman Aliyu Aliyu[1]., Hassan Aliyu[2]

[1]Department of Civil Engineering, Ahmadu Bello University, Zaria
[2]Department of Civil Engineering, Nuhu Bamalli Polytechnic, Zaria

ARTICLE INFO

Article History
Received: 20 July 2025
Accepted: 31 July 2025
Published: 31 July 2025

Corresponding Author:
Tasiu Ashiru Sulaiman
Department of Civil Engineering, Faculty of Engineering, Ahmadu Bello University, Zaria, Nigeria
tasiuashirusulaiman@gmail.com

ABSTRACT

To encourage sustainable development, it is crucial to explore alternative materials from agricultural or industrial sources that can reduce construction expenses and improve concrete strength. This research focuses on utilizing Sesame straw ash (SSA), as a partial replacement for cement in production of eco-friendly concrete. The study investigated the effects of Sesame straw ash (SSA) on concrete with substitutions of 0, 5, 10, 15, 20, and 25 % relative to the cement weight. The workability of the concrete along with its compressive, splitting tensile, and flexural strengths were assessed with varying SSA proportions. Results showed that adding SSA decreases the workability and strengths of concrete. However, it was noted that the strengths of SSA-modified concrete generally improve with longer curing time. The developed models had high values of R^2 as 0.9846, 0.9903 and 0.9910 for compressive, splitting tensile and flexural strength respectively. The discrepancy between the predicted and actual values for all responses was found to be under 5 %, demonstrating excellent correlation between predicted and real results in optimal mixing configurations. The ideal mix of 0 % SSA and a curing age of 90 days achieved the maximum compressive strength of 28.294 MPa and a splitting tensile strength of 3.949 MPa and flexural strength of 3.99 MPa. It was concluded that the developed models were suitable for estimating the strengths of the concrete.

***Keywords**:* *Sesame straw ash (SSA) · Cement · Workability · Compressive Strength · Flexural Strength · · Pozzolana*

1. Introduction

In numerous developing nations, the rapid rise in the cost of traditional construction materials has resulted in heightened overall expenses for civil engineering and building initiatives. To reduce material costs and the total financial burden of construction and civil engineering projects, various investigations have concentrated on utilizing affordable, locally available materials, such as byproducts from the agricultural and industrial sectors, as alternatives to cement in infrastructure projects [1]. The use of supplementary cementing materials (SCM) in concrete is essential for altering its properties. This research intends to assess the effectiveness of Sesame straw ash (SSA) as a supplementary cementitious material in concrete production, with the goal of enhancing the economic conditions of local farmers by repurposing waste materials as a more economical alternative to traditional admixtures, thus lowering construction costs and tackling the environmental issues related to the buildup of unmanaged waste. Despite the limited studies focused on the application of Sesame straw ash (SSA) in concrete, there is existing research regarding the usage of ashes from agricultural residues. A study by Orame *et al.*, [2] indicated that Sesame Plant Mucilage (SPM) has a total composition of SiO_2, Al_2O_3, and Fe_2O_3 of 25.58 %. The results illustrated that, following 28 days of curing, concrete mixed with varying proportions of Sesame mucilage displayed higher compressive strength than the control mixture, recording values of 33.2 N/mm^2, 31.0 N/mm^2, and 30.8 N/mm^2 for 1.0 %, 1.5 %, and 2.0 % Sesame mucilage concentrations, respectively. The authors concluded that adding sesame mucilage enhanced both flexural and split tensile strengths, yielding results that surpassed those of the control specimen through all curing periods. Research conducted by Elmardi *et al.,* [3] found that incorporating Sesame stalks fiber (SSF) into the concrete mix resulted in decreased strength of SSF-concrete as the SSF content increased; however, this inclusion resulted in improved resistance to cracking in the concrete. A study by Sulaiman *et al.*, [4] noted that the addition of sesame straw ash (SSA) diminished the flow (workability) and compressive strength of mortar, while simultaneously enhancing the soundness, setting times, and consistency of the SSA-cement paste. Nevertheless, the compressive strength of SSA-mortar saw improvement with an extended curing duration. Mohammed *et al.,* [5] employed response surface methodology to refine and characterize cast-in-situ alkali-activated pastes, revealing a strong correlation between predicted results and the experimental values gathered. The research showed that the best strengths were attained by mixing 100 percent GGBS with 11.19 percent solid sodium metasilicate in relation to the total weight of the primary components. In the study by Adamu *et al.*,[6] the water permeability and water absorption characteristics of the created pervious concrete were investigated, pinpointing the optimized variables that produced optimal durability performance as 0 % Rice Husk Ash (RHA) and 5 % calcium carbide waste (CCW) content. Garba et al., [7] utilized response surface methodology to optimize the integration of cement kiln dust, formulating predictive models for the strength and durability of self-compacting concrete, ultimately concluding that 10 % cement kiln dust (CKD) can act as a partial substitute for cement in self-compacting concrete. Garba et al., [8] using response surface methodology, established that a Styrofoam content of 0.547 % could be used to fabricate lightweight concrete after 28 days of curing. A research conducted by [9] indicates that the maximum concrete strength measured was 40.2 N/mm^2 and 46.02 N/mm^2 at 28 days and 120 days of curing with the addition of 2 % nanoparticles and 15 % Metakaolin, respectively. Ogork et al. [10] explored the effect of Groundnut husk ash (GHA) combined with rice husk ash in concrete, revealing that GHA has lower reactivity compared to RHA, with totals of Fe_2O_3, Al_2O_3, and SiO_2 at 26.06 % and 80.33 %, respectively. Aboshio et al. [11] reported that the slump of RHA-concrete decreased as the amount of RHA increased for both concrete grades produced; however, concrete strength improved with the addition of 5% RHA and 10 % RHA, with the most significant enhancement in strength occurring at 5 % RHA. They recommended that 5 % RHA be utilized as an admixture in concrete. Ogork et al., [10] found that the workability and characteristic strength of concrete decreased as the content of GHA-RHA increased, concluding that 15 % GHA-RHA is optimal for use in concrete.

This research focuses on utilizing agricultural waste ash, specifically Sesame straw ash (SSA), as a partial replacement for cement in creating eco-friendly concrete and also to reduce environmental challenges created by the wastes.

2. Materials and Methods

2.1 Materials

The cement used in this study was Dangote BlocMaster Portland limestone cement (PLC), which is categorized as grade 42.5R, exhibiting a moisture content of 1.81 % and a specific gravity of 3.16. The details regarding the composition of the cement oxides can be found in Table 2. The fine aggregate was obtained from the Zaria Local Government Area in Kaduna State, Nigeria, showing a silt content of 2 %, a specific gravity of 2.68, and a bulk density of 1737 kg/m^3. The coarse aggregate has a specific gravity of 2.68 along with a bulk density of 1425 kg/m^3. The sesame straw ash (SSA) was produced by burning sesame straw (SS) that was sourced from Jigawa State, Nigeria. This ash has a moisture content of 1.95%, a specific gravity of 2.69, and a loss on ignition (LOI) of 0.3 %. The water used in this study was potable and was sourced from the Department of Civil Engineering laboratory at ABU, Zaria, Kaduna State, Nigeria.

2.2 Methods

2.2.1 Characteristics of Concrete

The workability assessment was carried out on fresh concrete following the guidelines in [20]. The compressive strength test for SSA-concrete was executed according to [21]. Concrete samples were prepared and cured in potable water, with a total of 3 cubes measured for an average at each curing duration of 3, 7, 28, 56, and 90 days. Additionally, the splitting tensile strength test on SSA-concrete cylinders was performed in accordance with BS 1881-117: (1983). Concrete cylinders were cast, and three specimens were tested for an average at each curing period of 3, 7, 28, 56, and 90 days. The flexural strength test on SSA-concrete beams was conducted per BS 1881-118: (1983). Concrete beams were cast, and 3 samples were evaluated for an average across each curing period of 3, 7, 28, 56, and 90 days using the Avery-Denison universal testing machine.

2.2.2 Design of Experimental (DOE) for Blend Proportions using RSM

The methodology of Design of Experiments (DOE) incorporating Response Surface Methodology (RSM) was employed to identify the concrete mix proportions. The percentage of SSA ranged from 0 % to 25 %, while the curing durations were established at 3, 7, 28, 56, and 90 days. The software produced thirteen (13) potential mix combinations by defining lower and upper limits within the RSM DOE framework, as shown in Table 1. To enhance the precision, analysis, and error evaluation of the experiment, the central point was repeated five times using the Design Expert 13 software.

Table 1: Design of Experiment for Mixing Parameters and their Responses

Run	**Input Factors**		**Responses**		
	SSA (%)	**Curing Age (Days)**	**Compressive Strength (MPa)**	**Splitting Tensile Strength (Mpa)**	**Flexural Strength (Mpa)**
1	0	90	27.4	3.98	3.9
2	25	3	7.93	0.95	1.7
3	20	7	9.7	1.2	2
4	0	28	24.33	2.83	3.55
5	10	56	20.33	2.43	3.1
6	15	56	18.1	2.22	2.82
7	20	3	8.6	1.15	1.82
8	5	28	22.83	2.51	3.24
9	25	7	8.57	1.00	1.8
10	5	90	25.2	3.21	3.66
11	0	3	16.2	1.75	2.68
12	10	7	15.2	1.74	2.45
13	15	28	16.83	1.65	2.68

3. Results and Discussions

3.1 Oxide Composition of Cement and SSA

The findings from the XRF analysis conducted on cement and SSA are presented in Table 2. The oxide makeup of SSA reveals that the combined total of aluminium oxide (Al_2O_3), iron oxide (Fe_2O_3), and silicon oxide (SiO_2) is 28.92 %, which falls below the minimum threshold of 70 % set by ASTM C 618 for pozzolanic materials. The CaO content of 45.42 % in SSA indicates that it has some cementitious properties.

Table 2: Oxide Composition of Cement, SSA and RHA

Oxide	Na_2O	MgO	Al_2O_3	SiO_2	K_2O	CaO	TiO_2	Cr_2O_3	Fe_2O_3
Cement (%)	0.18	1.05	2.83	21.43	1 0.62	68.02	0.17	-	2.77
SSA (%)	1.08	3.55	1.82	20.83	8.02	45.42	1.47	0.01	6.27

3.2 Slump of Fresh SSA-Concrete

Figure 1 displays the slump values of concrete with different levels of SSA content. The results from the slump tests conducted on the fresh concrete, as depicted in Figure 1, show a decline in slump as the SSA content increases. This indicates that an increase in SSA quantity results in a decrease in the workability of the fresh concrete. This pattern supports the observation that SSA is more effective at absorbing water than cement, which aligns with the results obtained from the consistency tests conducted on SSA-cement paste. The decrease in slump can be linked to the greater surface area of SSA at a consistent water volume, which corresponds with the findings reported by [14]. Furthermore, this reduction can also be explained by the lower density of SSA in comparison to cement and its finer particle size. A comparable trend was noted by [15].

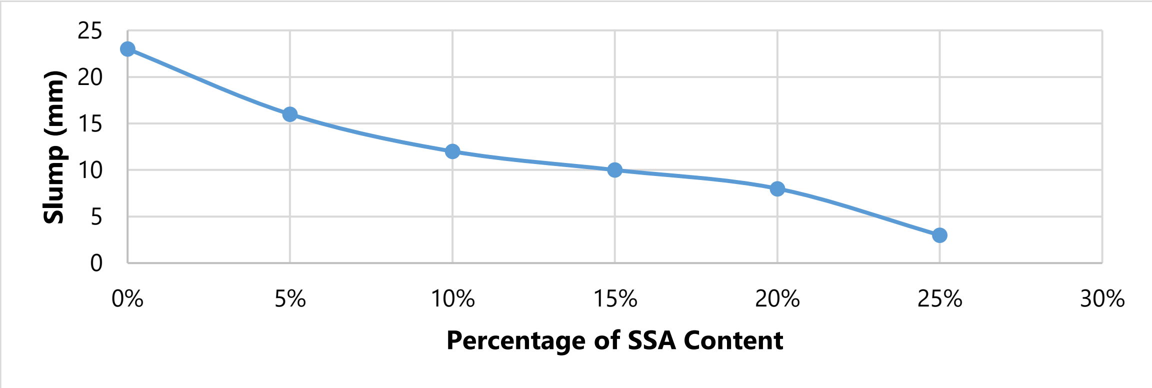

Figure 1. Relationship between Slump and percentage of SSA Content

3.3 Compressive Strength of SSA-Concrete

The strength of concrete is an essential property that is primarily applied in the design of structural concrete. Figure 2 displays the strength results of SSA-concrete. It has been noted that the strength of SSA-concrete diminishes as the percentage of SSA increases. The highest strength recorded was 27.4 N/mm^2 with 0 % SSA after 90 days of curing, while the lowest strength observed was 8.57 N/mm^2 with 25 % SSA after only 3 days of curing in fresh potable water. On the other hand, the strength of SSA-concrete improves with a longer curing duration. Significantly, at 28 days of curing, the strength of concrete containing 10 % SSA exceeded the target design strength of 20 N/mm^2. The decrease in concrete strength with higher SSA content may be linked to the reduced amount of cement available for hydration [18]. This might also be due to the dilution effects between cement and SSA [14]. In conclusion, the increase in compressive strength over prolonged curing periods can be attributed to the hydration processes involving cement and SSA.

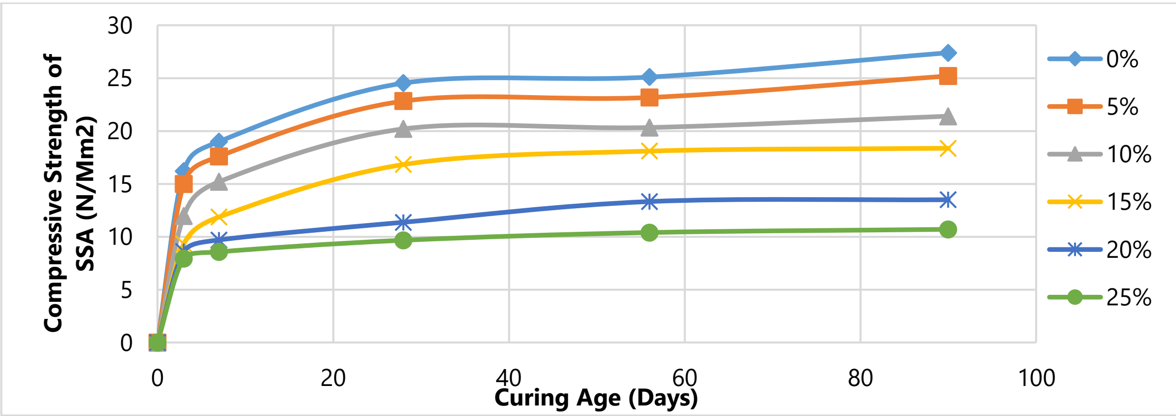

Figure 2. Relationship between Compressive Strength and Curing Age

3.4 Splitting Tensile Strength of SSA-Concrete

The findings regarding the splitting tensile strength of concrete made with different percentages of SSA are shown in Figure 3. As the SSA content increased, the splitting tensile strength of the SSA-concrete diminished. Conversely, this strength improved with prolonged curing time. The decline in splitting tensile strength in SSA-concrete is likely due to an increase in the pozzolanic reaction of silica from SSA and the calcium hydroxide released as a by-product of cement hydration, which results in an excess of calcium-silicate-hydrate, thereby enhancing binder efficiency, as noted by [9]. A similar trend was observed by [22].

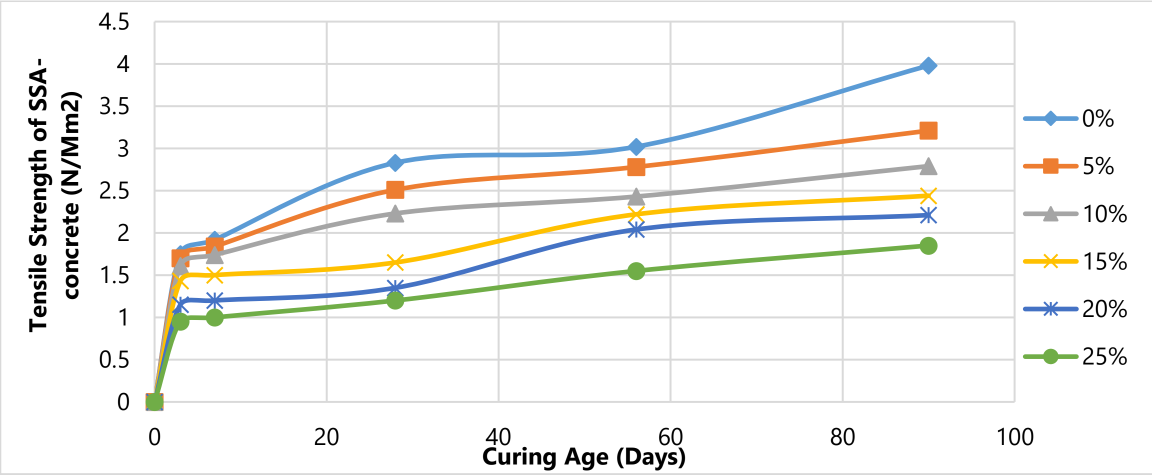

Figure 3. Relationship between Tensile Strength and Curing Age

3.5 Flexural Strength of SSA-Concrete

The results for the flexural strength of concrete with different percentages of SSA are shown in Figure 4. It was noted that with an increase in SSA content, the strength of the concrete tends to decrease, although it improves with longer curing durations. The measured flexural strength of the concrete varied from 3.9 N/mm² at 0 % SSA after 90 days of curing to 1.70 N/mm² at 25 % SSA after only 3 days of curing. The enhancement of concrete strength with prolonged curing time can be attributed to cement hydration and the pozzolanic reaction of SSA, as detailed by [24]. The decline in flexural strength with higher SSA content may result from the properties of SSA, where the dilution effect on cement and the limited strength development from the pozzolanic reaction contributed to the overall reduction in strength [24].

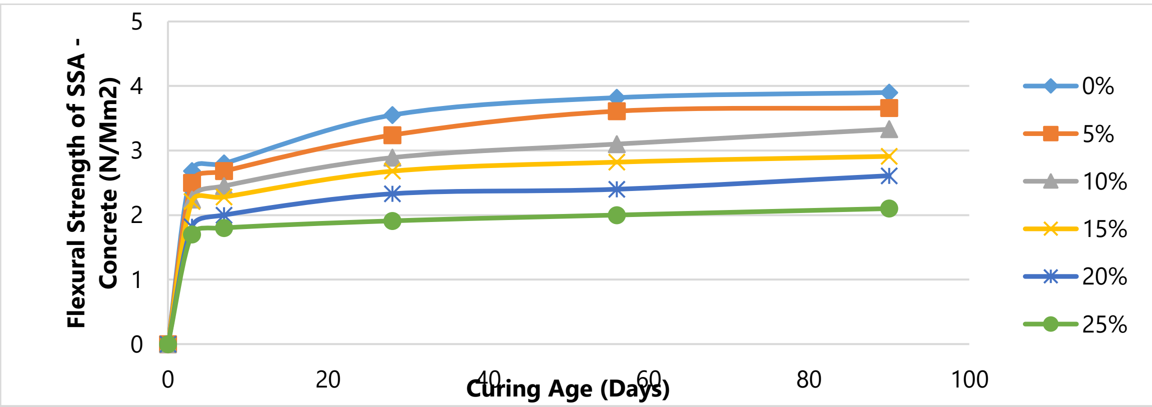

Figure 4. Relationship between Flexural Strength and Curing Age

3.6 Statistical Models Analysis

Response surface methodology (RSM) was utilized to analyze statistical models. It is defined as a mathematical and statistical approach applied in experimental design to determine relationships among various factors and to predict the optimal response by refining the associated parameter conditions. All developed models underwent statistical analysis and validation. The analysis was performed at a 5 percent significance level to assess the significance of experimental factors. For this analysis, compressive strength, splitting tensile strength, and flexural strength were treated as the dependent variables, while SSA and curing age were chosen as the independent factors. The analysis of variance was conducted to evaluate whether the factors had a significant impact on the response in accordance with the predetermined confidence level. A confidence level of 95 % was set, which indicated that the P-Value (probability level) should be less than 5 % ($p < 0.05$). A p-value lower than 0.05 indicates that the model is significant. According to Table 3, the models for compressive strength, split tensile strength and flexural strength showed p-values of < 0.0001, suggesting that these models are highly significant. Additionally, the selected models were based on the highest-order polynomial with significant terms unaffected by aliasing in the program. Moreover, the ANOVA results for the compressive, splitting tensile strength and flexural strength of SSA concrete are detailed in Table 3.

Table 3. ANOVA Model Analysis for the Responses

Parameter	Sum of Squares	Degree of Freedom	Mean Square	F-Value	P-Value	Remarks
Compressive Strength						
Model	550.88	5	110.18	89.80	<0.0001	Significant
A-SSA	55.73	1	55.73	45.43	0.0003	
B-Curing Age	6.20	1	6.20	5.05	0.0594	
AB	7.21	1	7.21	5.88	0.0458	
A^2	0.1255	1	0.1255	0.1023	0.7584	
B^2	25.04	1	25.04	20.41	0.0027	
Residual	8.59	7	1.23			
Cor Total	559.46	12				
Final Model	Quadratic					
Splitting Tensile Strength						
Model	10.15	5	2.03	142.29	<0.0001	Significant
A-SSA	1.02	1	1.02	71.54	<0.0001	
B-Curing Age	0.1836	1	0.1836	12.87	0.0089	
AB	0.2733	1	0.2733	19.14	0.0033	
A^2	0.0005	1	0.0005	0.0377	0.8515	
B^2	0.1842	1	0.1842	12.90	0.0088	
Residual	0.0999	7	0.0143			
Cor Total	10.25	12				
Final Model	Quadratic					
Flexural Strength						
Model	6.62	5	1.32	153.68	<0.0001	Significant
A-SSA	0.5940	1	0.5940	68.94	<0.0001	
B-Curing Age	0.1130	1	0.1130	13.12	0.0085	
AB	0.0625	1	0.0625	7.26	0.0309	
A^2	0.0000	1	0.0000	0.0038	0.9528	
B^2	0.2249	1	0.2249	26.10	0.0014	
Residual	0.0603	7	0.0086			
Cor Total	6.68	12				
Final Model	Quadratic					

In contrast, the F-values were significantly high, measuring at 89.80 for compressive strength, 142.29 for splitting tensile strength and 153.68 for flexural strength. Furthermore, P-values lower than 0.05 were obtained for all model responses, indicating that each generated model is significant at a 95% confidence level [16, 17].

3.7 Fit Statistical Analysis

The fit statistics for the models assessing compressive strength and splitting tensile strength are outlined in Table 4. The R^2 coefficients were found to be impressively high, specifically 0.9846 for compressive strength, 0.9903 for splitting tensile strength and 0.9910 for flexural strength. Additionally, Table 4 indicates that the difference between the predicted R^2 values and the adjusted R^2 values is less than 0.2, demonstrating a strong correlation. Moreover, the models' signal-to-noise ratio, adequacy, and effectiveness were analyzed using Adequate Precision (AP). To be considered effective, the AP value must be greater than 4 [16]. The findings show that the AP values do exceed 4, suggesting that the model can effectively support the design process. Therefore, based on the results presented in Table 4, it can be concluded that the developed models are not only effective but also skilled in modeling, optimizing, and predicting the compressive strength, splitting tensile strength and flexural strength of concrete blended with SSA content.

Table 4. Statistical Model Fit Analysis

Fit Statistics	**Compressive Strength (MPa)**	**Splitting Tensile Strength (MPa)**	**Flexural Strength (MPa)**
R^2	0.9846	0.9903	0.9910
Adjusted R^2	0.9737	0.9833	0.9845
Predicted R^2	0.9012	0.9352	0.9330
Coefficient of Variance (%)	6.50	5.83	3.41
Standard Deviation	1.11	0.1195	0.0928
Mean	17.03	2.05	2.72
Adequate Precision	27.7856	36.952	36.547

Additionally, the response surface methodology models for the compressive strength, splitting tensile strength and flexural strength were indicted in equations 1, 2 and 3 respectively.

$$\textbf{Compressive Strength} = 15.739-0.3063*\mathbf{A}+0.3767*\mathbf{B}-0.0063*\mathbf{AB}-0.00213*\mathbf{A}^2-0.00264*\mathbf{B}^2 \quad (1)$$

$$\textbf{Splitting Tensile Strength} = 1.689-0.0278*\mathbf{A}+0.0454*\mathbf{B}-0.00123*\mathbf{AB}-0.00014*\mathbf{A}^2-0.000226*\mathbf{B}^2 \quad (2)$$

$$\textbf{Flexural Strength} = 2.623-0.04093*\mathbf{A}+0.0377*\mathbf{B}-0.000587*\mathbf{AB}-0.000034*\mathbf{A}^2-0.00025*\mathbf{B}^2 \quad (3)$$

Where **A** and **B** are the SSA content and curing age respectively.

3.8 Model Diagnostic Plots

The residuals' probability and normal distribution plots for both the compressive strength, splitting tensile strength and flexural strength models are shown in Figures 5, 6 and 7, respectively. The arrangement of the residual points along a straight line in these figures reinforces the trustworthiness of the regression models [18, 19]. The closeness of the data points to the equality line reflects the dependability of the models. An analysis of Figures 5, 6 and 7 demonstrates that the predicted and actual values for the compressive strength, splitting tensile strength and flexural strength models are regularly aligned along the line, indicating a well-structured design that shows the models successfully predicted the results. This balanced arrangement emphasizes the models' suitability and precision, as it aligns closely with the actual laboratory data collected [23].

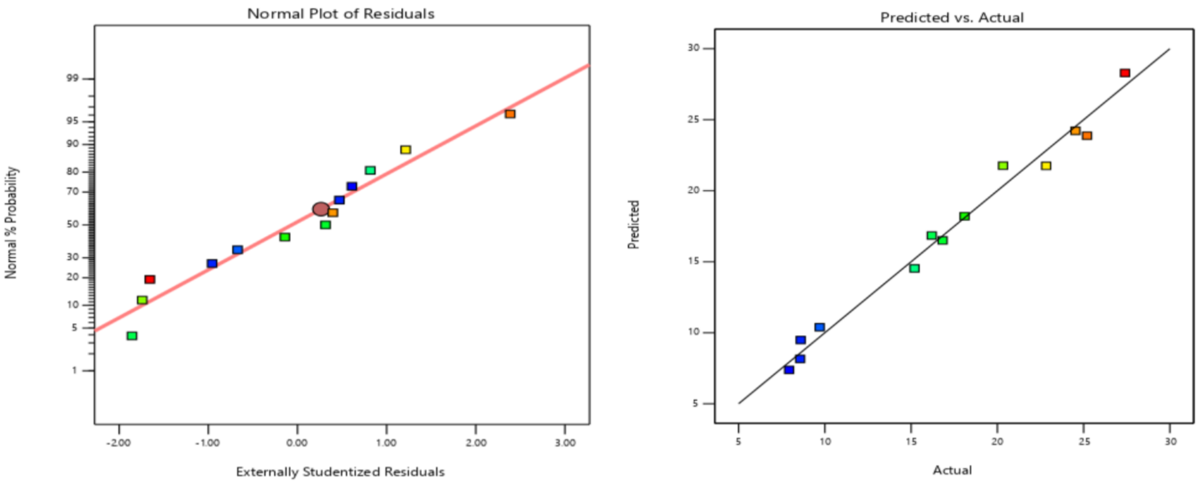

(a) (b)

Figure 5. Plot a and b are Diagnostics plots for the Compressive Strength

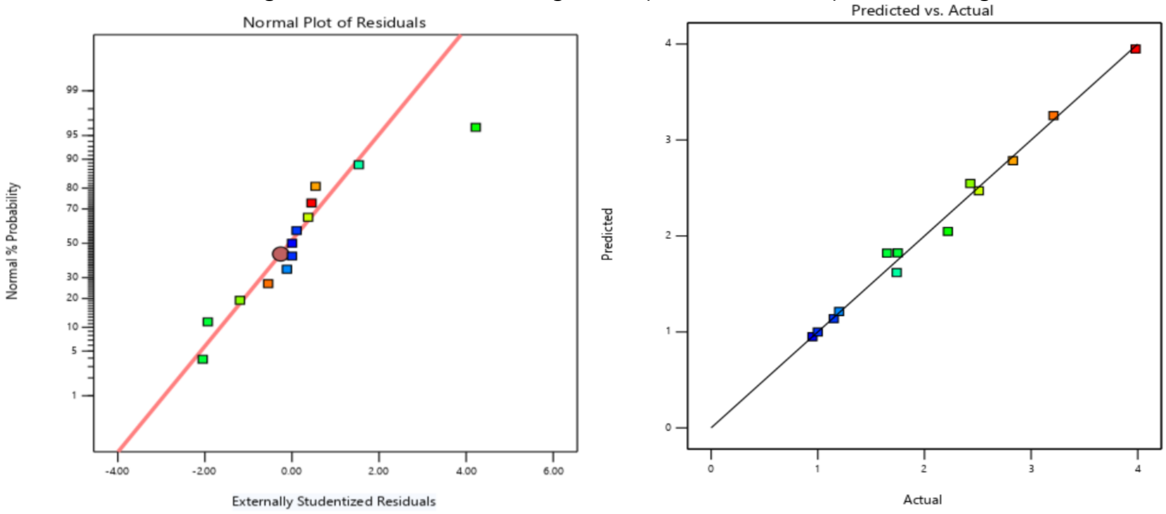

(a) (b)

Figure 6. Plot a and b are Diagnostics plots for the Splitting Tensile Strength

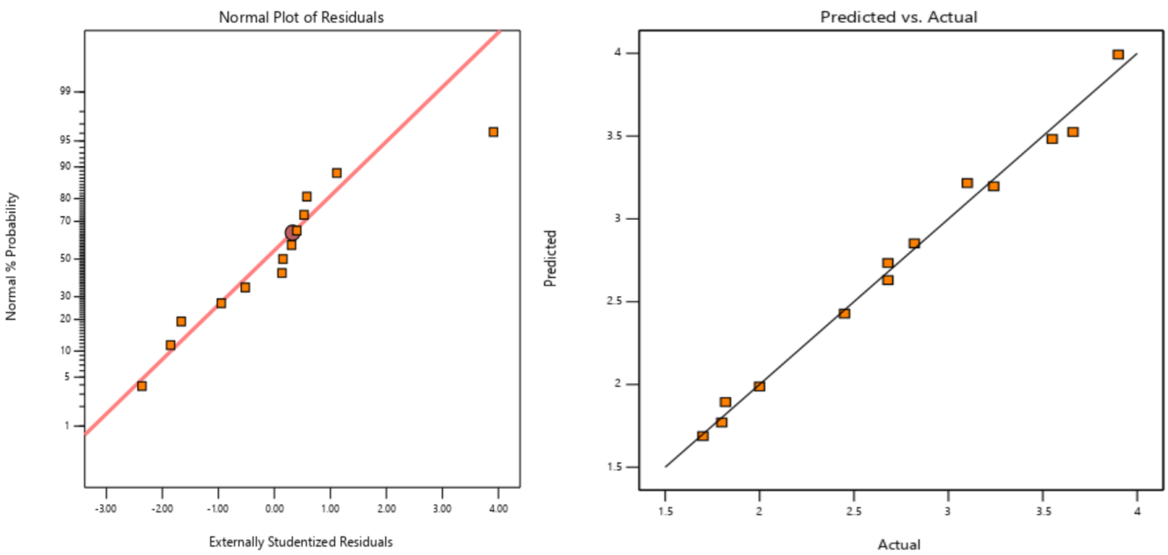

(a) (b)

Figure 7. Plot a and b are Diagnostics plots for the Flexural Strength

From an alternative perspective, the overarching impacts of SSA content and curing age on the outcomes were shown in Figures 8, 9 and 10 which illustrate the compressive strength, splitting tensile strength and flexural strength respectively. The diagnostic two-dimensional and three-dimensional plots displayed in Figures 8, 9 and 10 indicated that as the SSA content rose, the compressive strength, splitting tensile strength and flexural strength of the concrete decreased. In contrast, the strengths increased as the curing age advanced.

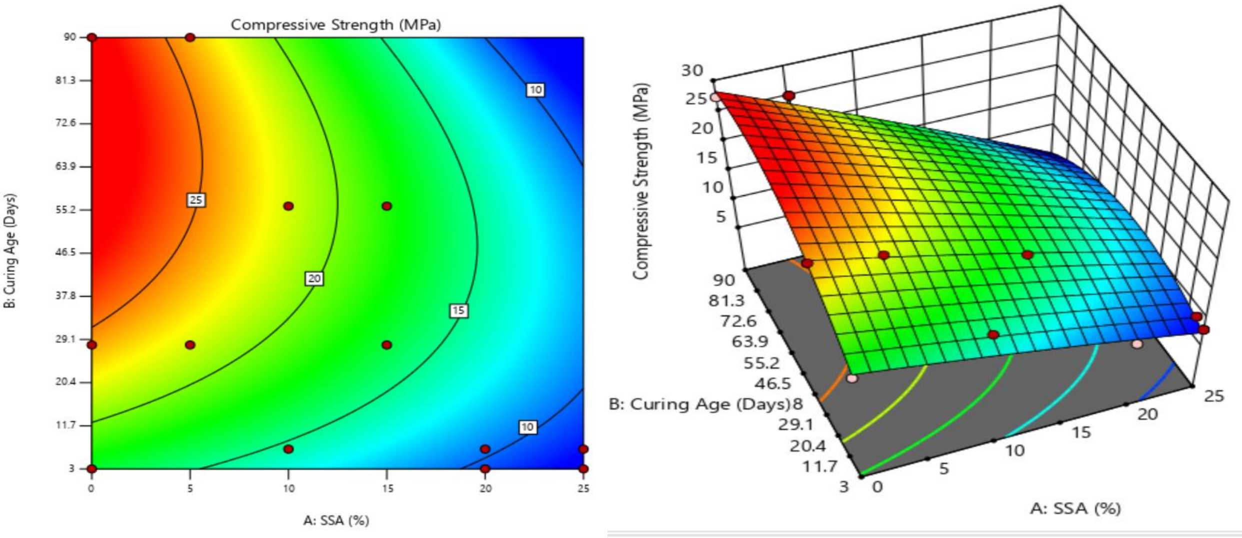

(a) (b)

Figure 8. Plots of the Compressive Strength of Concrete (a) 2D (b) 3D

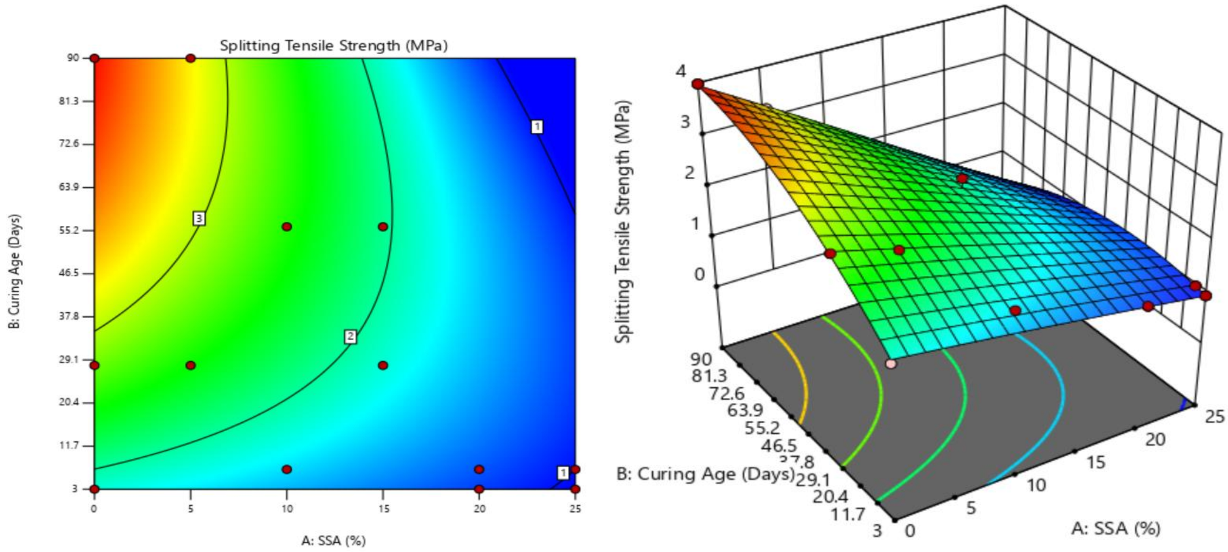

(a) (b)

Figure 9. Plots of Splitting Tensile Strength of Concrete (a) 2D (b) 3D

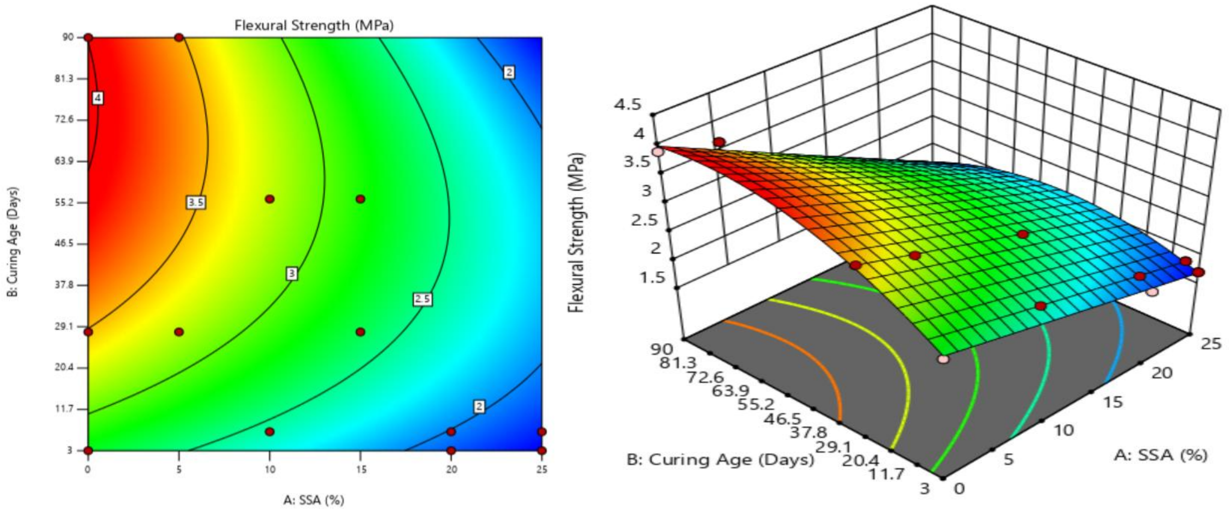

(a) (b)

Figure 10. Plots of the Flexural Strength of concrete (a) 2D (b) 3D

3.9 Models Numerical Optimization

The accuracy of the models and the achievement of specific goals were attained through a numerical optimization technique. The main goal is to improve the compressive strength, splitting tensile strength and flexural strength of concrete while keeping the SSA content and curing duration within defined limits. The input variables and the responses recorded during the optimization process are depicted in Figure 9. The optimization results identified the best parameters for enhancing and predicting the compressive, splitting tensile strength and flexural strength of concrete. Based on the results, the optimal input factors to achieve the desired performance were 0% SSA and a curing duration of 90 days. Moreover, the maximum compressive strength, splitting tensile strength and flexural strength reached with these parameters were 28.294 MPa, 3.949 MPa and 3.99 MPa respectively.

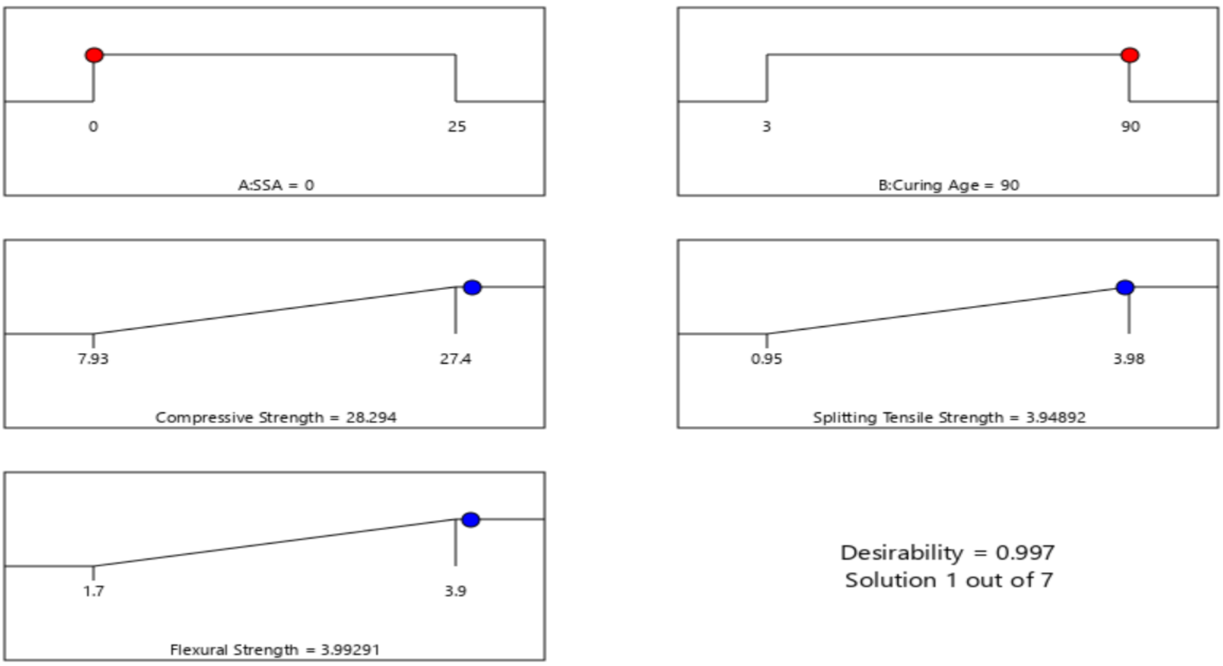

Figure 11. Ramps Numerical Optimization Analysis

3.10 Optimization and Verification

The objective of the optimization was to determine the most effective combination of SSA and curing age to improve the concrete's performance. Table 5 exhibits the optimized variable range and results. A numerical technique was employed to conduct the multi-objective optimization, focusing on reaching target values for SSA and curing age to maximize the compressive, splitting tensile strengths and flexural strength of concrete within the defined range. Additionally, the outcomes of the numerical optimization for the established models are displayed in Table 5. Moreover, seven separate solutions were generated from the responses, and the optimal mix was selected based on the highest desirability score. As a result, a mixture of 0% SSA and a curing age of 90 was found to achieve the maximum compressive, splitting tensile strengths and flexural strength within the defined range, yielding a combined desirability score of 0.997, as illustrated in Figure 11, which shows the ramps for numerical optimization. An additional set of experiments was conducted to verify the validity of the optimization results and the response models using the refined mix proportion to confirm the optimized mix proportion within the design mix. Equation 1 was used to calculate the percentage error between the experimental and predicted values. The percentage error differences indicated in Table 6 were found to be below 5 % for almost all evaluated responses, suggesting that the predicted values from the developed models are in close agreement with the experimental values.

$$Error(\%) = \frac{Experimental - Predicted}{Experimental}\ x\ 100 \quad (1)$$

Table 5: Optimization Bench Mark

Variables and Reponses	Purposes	Lower Limits	Upper Limits
SSA	In Range	0	25
Curing Age	In Range	3	90
Compressive Strength	Maximize	7.93	27.4
Splitting Tensile Strength	Maximize	0.95	3.98
Flexural Strength	Maximize	1.7	3.9

Table 6: Model Verification

Responses	Solution	SSA	Curing Age	Predicted	Experimental	Error (100)
Compressive	1	0	28	24.22	24.53	1.264
Strength	2	15	56	18.19	18.1	-0.497
(MPa)	3	20	3	8.49	8.6	1.279
Splitting Tensile	1	0	28	2.783	2.83	1.661
Strength	2	15	56	2.19	2.22	1.351
(MPa)	3	20	3	1.137	1.15	1.130
Flexural	1	0	28	3.483	3.55	1.887
Strength	2	15	56	2.836	2.82	-0.567
(MPa)	3	20	3	1.866	1.82	-2.527

4. Conclusions

The following deductions were made in light of the findings

i. Sesame straw ash (SSA) has a sum total of aluminium oxide (Al_2O_3), silicon oxide (SiO_2) and iron oxide (Fe_2O_3) as 28.92 % which is less than the lower limit of 70 % highlighted by ASTM C 618 for pozzolana and concluded to be a low reactive pozzolana. The addition of SSA led to a reduction in workability, compressive strength, splitting tensile strength and flexural strength of SSA concrete, although the strengths improved as the curing age increased.

ii. The generated models displayed excellent correlation, predictability, and alignment between the predicted and actual values, evidenced by high R^2 values and low P values, confirming their suitability for predictions.

iii. It was noted that the percentage error between the predicted and actual values for all responses was less than 5 %, suggesting a strong agreement between predicted and actual results under optimal mixing conditions.

iv. The optimal composition of 0 % SSA and a curing age of 90 % yielded the highest compressive strength of 28.294 MPa, splitting tensile strength of 3.949 MPa and flexural strength of 3.99 MPa respectively.

REFERENCES

[1] Ogork, E. N. and Ayuba, S. (2014). Influence of Sawdust Ash (SDA) as Admixture in Cement Paste and Concrete. *International Journal of Innovative Science, Engineering and Technology*, Vol. 1 No. 10. pp: 736-743. www.ijiset.com

[2] Orame, A. P., Abdulazeez, A. S. and Kolawole, M. A. (2020). An explorative study on the suitability of Sesame Plant Mucilage (Sesamum Indicum) as Admixture in Concrete. *International Journal of Engineering Applied Science and Technology*, Vol. 4, No. 11, pp: 574-581

[3] Elmardi, M. A., Kbbashe, A. I., Alkhair, O. A., Abdelmagid, T. I. (2021). The Effect of Adding Sesame Stalks Fibers to Concrete Mixture. *International Research Journal of Modernization in Engineering Technology and Science*, Vol. 3, No. 3, pp 1402 – 1409.

[4] Sulaiman, T. A., Mohammed, A., Aliyu, I., Ja'e, I. A., Wada, S. A. (2020). Assessment of Sesame Straw Ash as Partial Replacement of Cement in Mortar. *Proceedings of the Materials Science and Technology Society of Nigeria (MSN), OAU, Ile-Ife*, Nigeria. Vol. 1, pp: 40-45.

[5] Mohammeda, B.S., Harunaa,S., Abdul Wahaba, M. M., Liew, M. S. (2019). Optimization and characterization of cast in-situ alkali-activated pastes by response surface methodology. *Construction and Building Materials,* 225, 776-787. https://doi.org/10.1016/j.conbuildmat.2019.07.267

[6] Adamu, M., Ayeni, K. O., Haruna, S. I., Mansur, Y. E. I., Haruna, S. (2021). Durability Performance of Pervious Concrete Containing Rice Husk Ash and Calcium Carbide: A Response Surface Methodology Approach. *Case Studies in Construction Materials*. 14, e00547. https://doi.org/10.1016/j.cscm.2021.e00547.

[7] Garba, I., Amartey, Y. D., Sulaiman, T. A., Yau, Y., Sabari, A. A., Abdullahi, M. (2024a). Optimization of Cement Kiln Dust Incorporation and Development of Predictive Models for Strengths and Durability of Self-Compacting Concrete. UNIZIK Journal of Engineering and Applied Sciences, Vol. 3, No. 5, pp: 1370-1381

[8] Garba, I., Sulaiman, T. A., Aliyu, I., Kaura, J. M., Yau, Y., Yusuf, S. (2024). Predictive Models and Optimisation of Strengths and Durability of Self-Compacting Concrete Admixed with Styrofoam. *FUOYE Journal of Engineering and Technology*, 9(4): 686-692

[9] Lawan, A., Dugguh, L. N., Amartey, Y. D., and Ejeh, S. P. (2020). Properties of Concrete Containing Metakaolin and Nanoparticles from Rice Husk. *Journal of Scientific Research, Ahmadu Bello University, Zaria-Nigeria,* Vol. 19, No. 2, pp: 39-47.

[10] Ogork, E. N, Uche, O. A, and Elinwa, A. U. (2015). Characterization of groundnut Shell Ash (GSA) admixed with Rice Husk Ash (RHA) in cement paste and concrete. Advanced Materials Research, Vol. 11 No.19, pp 662-671. DOI:10.4028

[11] Aboshio, A., Ogork, E. N., and Balami, D. A. (2009). Rice Husk Ash as Admixture in Concrete. *Journal of Engineering and Technology (JET)* Vol.4, No. 2, pp: 95-101.

[12] BS 1881, Part 117 (1983): Method of determination of tensile splitting strength of concrete cylinders. British Standard Institution, London

[14] Sulaiman, T. A., Ja'e, A. I., Yau, Y., Garba, I., Abdurrahman, A. A., Maikanti, I. I. (2024). Influence of Sesame Husk Ash on Compressive Strength and Durability of Mortar. *2nd International Conference of Environmental Sciences (ICES 2024)*, pp: 114-123.

[15] Sulaiman, T. A. and Aliyu, I. (2020). Combined Effect of Rice Husk Ash and Cement Kiln Dust as Cement Replacement Materials in Concrete. *FUDMA Journal of Sciences (FJS),* Vol. 4 No. 1, pp 446 – 452.

[16] Garba, I., Sulaiman, T. A., Yau, Y., Kadandan, I. M., Solomon, B. (2024). Mechanical Performance of Sisal Fibre-Modified Self Compacting Concrete: A Comprehensive Study. *Journal of Sustainable Engineering and Technology* Vol. 1, No. 2, pp: 129 – 140

[17] Haruna, S., Mohammed, B. S., Wahab, M. M. A., Haruna, A. (2020). Compressive Strength and Workability of High Calcium One Part Alkali Activated Mortars using Response Surface Methodology. *2nd International Conference of Civil & Environmental Engineering: IOP Conf.series: Earth and Environmental Science* 476. doi:10.1088/17755-1315/476/1/01/2018.

[18] Garba, I., Sulaiman, T. A., Aliyu, I., Kaura, J. M., Yau, Y., Suleiman, Y. (2024c). Predictive Models and Optimization of Strengths and Durability of Self-Compacting Concrete Admixed with Styrofoam. *FUOYE Journal of Engineering and Technology,* Vol. 9, No. 4, pp: 686-692.

[19] Sulaiman, T. A., Ja'e, I. A., Ja'e, Yau, Y., Abdulkadir, I. (2019). Assessment of the Combined Effect of Groundnut Shell Ash (GSA) and Saw Dust Ash (SDA) as Partial Replacement for Cement in Mortar. *Proceedings of Material Science and Technology Society of Nigeria (MSN), Kaduna Chapter*, pp: 59-64.

[20] BS EN 12350, Part 2, (2009). Slump Test, British Standard Institution, London.

[21] BS EN 12390, Part 3, (2009). Method for Determination of Compressive strength of Concrete Cubes, British Standard Institution, London.

[22] Ettu, L. O., Anyaogu, L., and Diboyesuku, I.D. (2021). Investigation of the Tensile and Flexural Strengths of Concrete Containing Rice Husk and Saw Dust Ashes. *International Journal of Scientific & Engineering Research*, Vol. 12, No. 7, pp: 1183-1188.

[23] Jae, I. A., Sulaiman, T. A., Amartey, B. H. S., Abdurrahman, A. A., Iliyasu, I., Umar, A. U. (2024). Predictive Evaluation and Optimization of Mechanical Properties of Kenaf-Polypropylene Fibre Reinforced Concrete Using Response Surface Methodology. *Proceedings of the 2nd International Conference of Environmental Sciences (ICES 2024)*. Pp:367-376

[24] Ogork, E. N. and Uche, O. A. (2014). Effects of Groundnut Husk Ash (GHA) in Cement Paste and Mortar. *International Journal of Civil Engineering and Technology (IJCIET)*, Vol. 5, No. 10, pp: 88-95.